Publication Year	2023
Acceptance in OA	2025-03-03T13:24:23Z
Title	GRB 221009A: Discovery of an Exceptionally Rare Nearby and Energetic Gamma-Ray Burst
Authors	Williams, Maia A., Kennea, Jamie A., Dichiara, S., Kobayashi, Kohei, Iwakiri, Wataru B., Beardmore, Andrew P., Evans, P. A., Heinz, Sebastian, Lien, Amy, Oates, S. R., Negoro, Hitoshi, Cenko, S. Bradley, Buisson, Douglas J. K., Hartmann, Dieter H., Jaisawal, Gaurava K., Kuin, N. P. M., Lesage, Stephen, Page, Kim L., Parsotan, Tyler, Pasham, Dheeraj R., SBARUFATTI, Boris, Siegel, Michael H., Sugita, Satoshi, Younes, George, AMBROSI, Elena, Arzoumanian, Zaven, BERNARDINI, Maria Grazia, CAMPANA, Sergio, CAPALBI, Milvia, Caputo, Regina, D'AI', Antonino, D'AVANZO, Paolo, D'ELIA, Valerio, De Pasquale, Massimiliano, Eyles-Ferris, R. A. J., Ferrara, Elizabeth, Gendreau, Keith C., Gropp, Jeffrey D., Kawai, Nobuyuki, Klingler, Noel, Laha, Sibasish, MELANDRI, Andrea, Mihara, Tatehiro, Moss, Michael, O'Brien, Paul, Osborne, Julian P., Palmer, David M., PERRI, Matteo, Serino, Motoko, Sonbas, E., Stamatikos, Michael, Starling, Rhaana, TAGLIAFERRI, Gianpiero, Tohuvavohu, Aaron, Zane, Silvia, Ziaeepour, Houri
Publisher's version (DOI)	10.3847/2041-8213/acbcd1
Handle	http://hdl.handle.net/20.500.12386/36382
Journal	THE ASTROPHYSICAL JOURNAL LETTERS
Volume	946

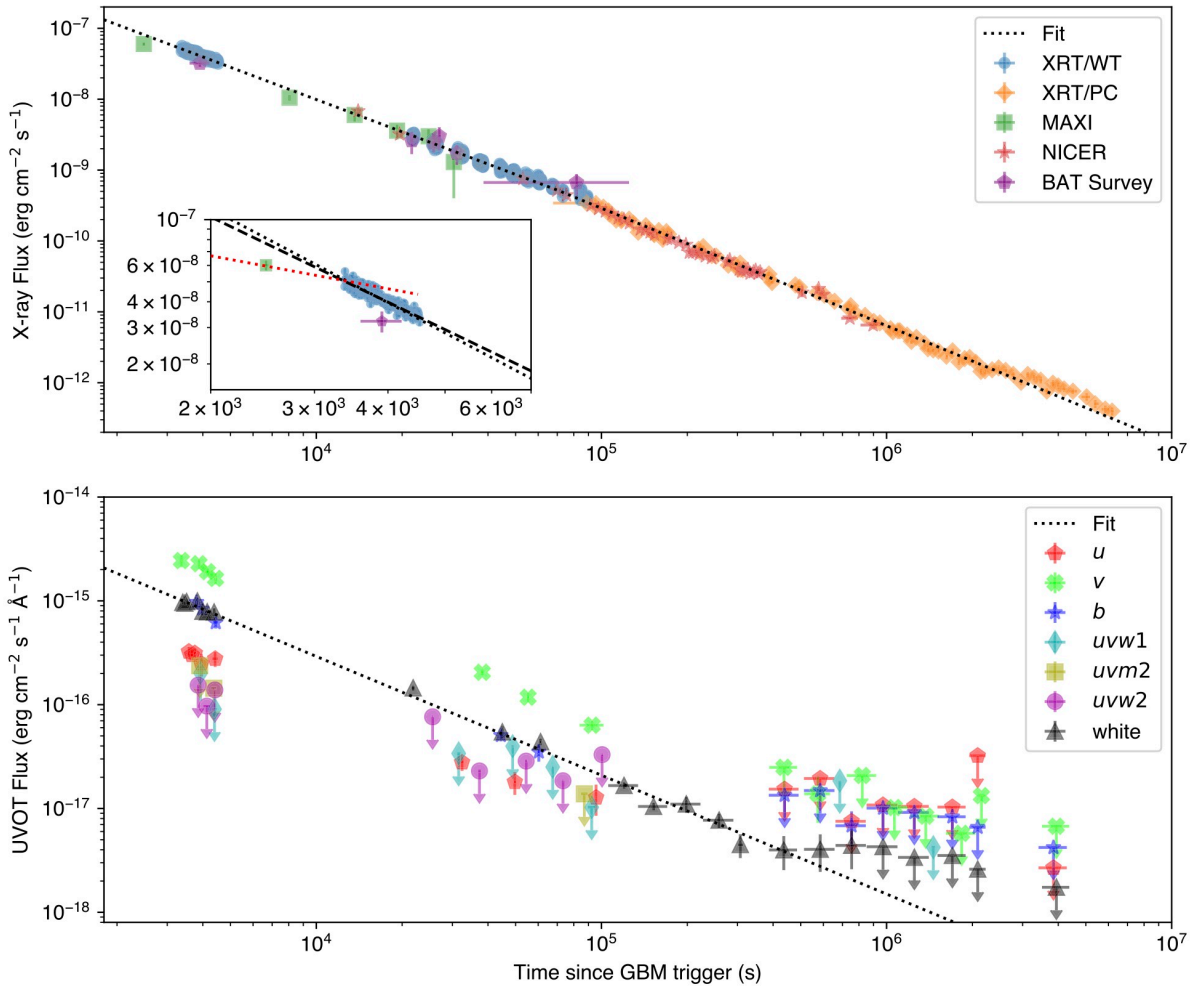

Figure 2. Combined X-ray and UV–optical light curve of GRB 221009A. The upper panel shows observed X-ray flux from MAXI, NICER, XRT (all 0.3–10.0 keV), and BAT (14–195 keV). BAT data are taken from detections of the afterglow in Survey data; note that the final BAT data point combines all observations integrated over 1 day. The dotted line shows a broken power-law fit to the MAXI, NICER, and XRT data. The inset figure shows the first MAXI, BAT, and XRT data, with the black dashed line indicating a fit to the XRT data alone, and red dashed line a fit between the first MAXI point and the first XRT detection. The lower panel shows 7 filter optical and UV data from UVOT as obtained after the subtraction of late-time template images. The dashed line shows a power-law fit to the white band data.

automated XRT analysis (Evans et al. 2007, 2009) needs some modification. For PC mode, this is relatively simple, as we have full 2D imaging, and the innermost rings were reasonably well separated from the GRB itself. We restricted the source region to a radius of 20 pixels (47″), and extracted a combined background from four regions[37] across the detector, which are as free from dust contamination as possible (identified from a stacked image of all PC-mode data). In order to quantify the impact of dust contamination in the background, we calculated the background rate in these regions, and found an average value of 1.6×10^{-6} ct s^{-1}, which is consistent with historical values (Evans et al. 2023). During the first ∼5 days, dust ring contamination caused a 4–10 times elevation of the background rate. However, during this period, the afterglow of GRB 221009A is 30–50 times brighter than the background level, meaning the effect is negligible.

For WT mode, this is more problematic since the CCD is read out in columns, rather than pixels. After investigating the variation in the echo contribution to WT-mode data, we modified the default WT extraction regions to minimize its impact (see Appendix B). We found that the WT flux is accurate to ∼6%. We further verified this by extracting a light curve using only data above 4 keV, where dust scattering becomes less efficient, given the roughly ν^{-2} dependence of the scattering cross section; only minimal changes in the light-curve shape are observed. On the other hand, the dust has more significant impact on the WT spectra (Appendix B), resulting in an increase in the best-fit photon index up to ∼7% and a significant increase to the best-fit absorption column (up to ∼27%).

We modified the settings for the automated light curve[38] to limit the source extraction region to 20 pixels radius, and to use

[37] Background region coordinates: R.A./decl. = 288.°3403, 19.°7616, radius = 47″, R.A./decl. = 288.°2986, 19.°7073, radius = 41″, R.A./decl. = 288.°2345, 19.°8409, radius = 34″, and R.A./decl. = 288.°1830, 19.°7734, radius = 29″.

[38] https://www.swift.ac.uk/xrt_curves/01126853/